

## SO(4) Theory of Antiferromagnetism and Superconductivity in Bechgaard Salts

Daniel Podolsky, Ehud Altman, Timofey Rostunov, and Eugene Demler

*Department of Physics, Harvard University, Cambridge, Massachusetts 02138, USA*

(Received 18 March 2004; published 6 December 2004)

Motivated by recent experiments with Bechgaard salts, we investigate the competition between antiferromagnetism and triplet superconductivity in quasi-one-dimensional electron systems. We unify the two orders in an SO(4) symmetric framework, demonstrating the existence of such symmetry in one-dimensional Luttinger liquids. SO(4) symmetry strongly constrains the phase diagram, leading to coexistence regions of antiferromagnetic, superconducting, and normal phases, as observed in (TMTSF)<sub>2</sub>PF<sub>6</sub>. We predict a sharp neutron scattering resonance in superconducting samples.

DOI: 10.1103/PhysRevLett.93.246402

PACS numbers: 71.10.Pm, 74.25.Dw, 74.70.Kn

A common feature of many strongly correlated electron systems is the proximity of a superconducting state to some kind of magnetically ordered insulating state. Examples include organic materials [1,2], heavy fermion superconductors [3,4], and high  $T_c$  cuprates [5]. Several theoretical analyses suggest that a strong repulsion between the two orders plays an important role in determining the phase diagram and low energy properties of these materials [6]. The idea of competing orders was developed into the SO(5) theory of high  $T_c$  superconductivity of Zhang [7]. SO(5) symmetry has also been applied to study the competition of ferromagnetism and  $p$ -wave superconductivity in Sr<sub>2</sub>RuO<sub>4</sub> [8], and antiferromagnetism and  $d$ -wave superconductivity in  $\kappa$ -BEDT-TTF salts [9].

In this Letter we consider the interplay of antiferromagnetism (AF) and triplet superconductivity (TSC) in quasi-one-dimensional (Q1D) electron systems. Our study is motivated by Q1D Bechgaard salts (TMTSF)<sub>2</sub>X. The most studied material from this family, (TMTSF)<sub>2</sub>PF<sub>6</sub>, is an antiferromagnetic insulator at ambient pressure and a superconductor at high pressures [10–13]. The symmetry of the superconducting order parameter in (TMTSF)<sub>2</sub>PF<sub>6</sub> is not fully established, but there is strong evidence of spin-triplet electron pairing:  $T_c$  is strongly suppressed by disorder [14]; the critical field  $H_{c2}$  along the chains exceeds the paramagnetic limit [15]; the electron spin susceptibility in Knight shift measurements does not decrease below  $T_c$  [16]. In another member of this family, (TMTSF)<sub>2</sub>ClO<sub>4</sub>, superconductivity is stable at ambient pressure and also shows signatures of triplet pairing [17]. Insulator to superconductor transition with applied pressure is also seen in (TMTSF)<sub>2</sub>AsF<sub>6</sub> [18].

The phase diagram of interacting electrons in 1D is obtained in Ref. [19] from bosonization and renormalization group (RG) analyses. At incommensurate filling, there is a phase boundary between spin density wave (SDW) and TSC phases when  $K_\rho = 1$  and  $g_1 > 0$  ( $K_\rho$  is the Luttinger parameter in the charge sector;  $g_1$  is the backward scattering amplitude). The starting point of our discussion is the observation that, in the absence of um-

klapp, 1D Luttinger liquids have an “isospin” SO(4)<sub>iso</sub> symmetry [20] at the SDW-TSC phase boundary. This is defined by the charge of left and right moving electrons,  $Q_\pm = \frac{1}{2} \sum_{ks} (a_{\pm,ks}^\dagger a_{\pm,ks} - \frac{1}{2})$ , and two new operators ( $r = \pm$ ):

$$\Theta_r^\dagger = r \sum_k a_{r,k\uparrow}^\dagger a_{r,-k\downarrow}^\dagger. \quad (1)$$

Here  $a_{\pm,ks}^\dagger$  creates right or left moving electrons of momentum  $\pm k_f + k$  and spin  $s$ . Combining these into  $J_x = (\Theta_r^\dagger + \Theta_r)/2$ ,  $J_y = (\Theta_r^\dagger - \Theta_r)/2i$ , and  $J_z = Q_r$ , we see that the generators satisfy two independent chiral SO(3) algebras,  $[J_a^r, J_b^{r'}] = i\delta^{r,r'} \epsilon^{abc} J_a^r$ . The product of left and right algebras yields the total isospin group SO(4)<sub>iso</sub>  $\approx$  SO(3)<sub>R</sub>  $\times$  SO(3)<sub>L</sub>. The Luttinger Hamiltonian at incommensurate filling,  $\mathcal{H}$ , generically commutes with the charge operators  $Q_\pm$ . Using a bosonized form of  $\mathcal{H}$ , one can show that, at  $K_\rho = 1$ ,  $\Theta_\pm$  also commute with  $\mathcal{H}$  [20,21]. Thus, SO(4)<sub>iso</sub> is an exact symmetry of  $\mathcal{H}$  at  $K_\rho = 1$ . In addition, for spin-symmetric interactions, which describe Bechgaard salts well [21,22], the system has SO(3)<sub>spin</sub> symmetry generated by the total spin  $S_\alpha = \frac{1}{2} \sum_{r,ks s'} a_{r,ks}^\dagger \sigma_{ss'}^\alpha a_{r,ks'}$ . Hence, for  $K_\rho = 1$ , i.e., the line separating SDW and TSC phases, the system has full SO(3)<sub>spin</sub>  $\times$  SO(4)<sub>iso</sub> symmetry. For Luttinger liquids at incommensurate filling, this symmetry always appears at the SDW-TSC phase boundary without fine-tuning.

This symmetry can be used to unify SDW and TSC order parameters. SDW order away from half-filling is described by a complex vector order parameter,

$$\Phi_\alpha = \sum_{kss'} a_{+,ks}^\dagger \sigma_{ss'}^\alpha a_{-,ks'}. \quad (2)$$

Q1D band structure restricts the orbital component of TSC order to lie in the interchain axis  $x$ ,  $\Psi(\mathbf{p}) \propto p_x$ . Thus, the TSC order parameter is also a complex vector,

$$\Psi_\alpha^\dagger = \frac{1}{i} \sum_{kss'} a_{+,ks}^\dagger (\sigma^\alpha \sigma_2)_{ss'} a_{-,-ks'}. \quad (3)$$

The four vector order parameters  $\text{Re}\Phi$ ,  $\text{Im}\Phi$ ,  $\text{Re}\Psi$ , and

$\text{Im}\Psi$  can be combined into a  $4 \times 3$  matrix,

$$P_{\bar{a}\alpha} = \begin{pmatrix} (\text{Re}\Psi)_x & (\text{Im}\Psi)_x & (\text{Re}\Phi)_x & (\text{Im}\Phi)_x \\ (\text{Re}\Psi)_y & (\text{Im}\Psi)_y & (\text{Re}\Phi)_y & (\text{Im}\Phi)_y \\ (\text{Re}\Psi)_z & (\text{Im}\Psi)_z & (\text{Re}\Phi)_z & (\text{Im}\Phi)_z \end{pmatrix}. \quad (4)$$

Each column [row] of  $\hat{P}$  transforms independently as a vector under the action of  $\text{SO}(3)_{\text{spin}}$  [ $\text{SO}(4)_{\text{iso}}$ ].

The  $\Theta_r$  operators are reminiscent of the  $\eta$  operator, which generates an  $\text{SO}(4)$  symmetry for the Hubbard model [23]. Unlike  $\eta$ , whose center of mass momentum is always the commensurate wave vector  $\pi$ ,  $\Theta_r$  have their momenta at the wave vectors  $\pm 2k_f$ . This is crucial for defining the symmetry at arbitrary electron density; in contrast,  $\text{SO}(4)$  in Ref. [23] applies only at half-filling.

Real materials are only Q1D and coupling between chains gives rise to finite temperature phase transitions. However, as long as 3D coupling is weaker than the intrachain tunneling and interactions, the nature of the ordered state is determined by the most divergent susceptibility within individual chains. Hence, for Q1D materials near the SDW-TSC boundary we expect to find  $K_\rho$  close to 1 and to find approximate  $\text{SO}(3)_{\text{spin}} \times \text{SO}(4)_{\text{iso}}$  symmetry. Then, the phase diagram in three spatial dimensions is obtained from a Ginzburg-Landau (GL) free energy whose form is strongly constrained by symmetry,

$$F = \frac{1}{2}(\nabla P_{\bar{a}\alpha})^2 + \bar{r}P_{\bar{a}\alpha}^2 + \delta r(P_{1\alpha}^2 + P_{2\alpha}^2 - P_{3\alpha}^2 - P_{4\alpha}^2) + \tilde{u}_1 P_{\bar{a}\alpha}^2 P_{\bar{b}\beta}^2 + \tilde{u}_2 P_{\bar{a}\alpha} P_{\bar{a}\beta} P_{\bar{b}\alpha} P_{\bar{b}\beta}. \quad (5)$$

This is the most general expression with  $\text{SO}(3)_{\text{spin}} \times \text{SO}(4)_{\text{iso}}$  symmetric quartic coefficients. We follow the common assumption that external control parameters, e.g., temperature and pressure, affect only quadratic coefficients. These are thus allowed to break the symmetry and tune the phase transition. For  $\delta r \neq 0$ , the symmetry is reduced to  $\text{SO}(3)_{\text{spin}} \times \text{SO}(2)_c \times \text{SO}(2)_t$ , where  $\text{SO}(2)_c$  is generated by the total charge  $Q = Q_+ + Q_-$ , and  $\text{SO}(2)_t$  is due to lattice translational symmetry [24].

At half-filling, umklapp scattering must be included. This applies to Bechgaard salts, where structural dimerization splits the conduction band into a full lower band and a half-filled upper band. Umklapp turns two right movers into left movers, and vice versa:

$$\mathcal{H}_3 = \frac{g_3}{2L} \sum a_{+,k+qs}^\dagger a_{+,p-qt}^\dagger a_{-,pr} a_{-,ks} + \text{H.c.} \quad (6)$$

This pins the phase of the SDW, reducing it to a real Néel vector  $\mathbf{N} = \text{Re}\Phi$  (for  $g_3 > 0$ ). There is still a direct AF-TSC transition at  $K_\rho = 1$  [1], but  $Q_+$  and  $Q_-$  are no longer conserved separately. Thus, the  $\text{SO}(4)_{\text{iso}}$  symmetry of the free energy is broken. However, to linear order in  $g_3$ ,  $\text{SO}(4)_{\text{iso}}$  is not broken all the way down to  $\text{SO}(2)_c$ . The contribution of  $\mathcal{H}_3$  to the free energy,  $\Delta F = \frac{g_3}{L} \times [(\text{Re}\Phi)^2 - (\text{Im}\Phi)^2]$ , preserves a residual  $\text{SO}(3)_{\text{iso}}$ , equal to the diagonal subgroup of  $\text{SO}(3)_R \times \text{SO}(3)_L$  [21]. The generators of  $\text{SO}(3)_{\text{iso}}$  are  $I_a = J_a^+ + J_a^-$ . Together

with spin, they define the symmetry  $\text{SO}(4) \approx \text{SO}(3)_{\text{spin}} \times \text{SO}(3)_{\text{iso}}$ .

The justification for considering small  $g_3$  is as follows. The bare value of  $g_3$  is proportional to dimerization, which is of order 1% in  $(\text{TMTSF})_2\text{PF}_6$  [25]. Furthermore, the GL energy depends on the renormalized value  $g_{3,\text{eff}}$  at the 1D–3D crossover scale, which is even smaller than the bare value of  $g_3$ . Umklapp is irrelevant inside the TSC phase, as well as on the AF-TSC boundary. Even in the AF phase, where umklapp is relevant,  $g_3$  flows near zero before diverging, and this divergence may be cut off by the onset of 3D coupling. Thus, everywhere near the AF-TSC boundary, we can assume that  $g_{3,\text{eff}}$  is small.

$\text{SO}(4)$  symmetry unifies AF and TSC orders, which are now combined into a  $3 \times 3$  tensor order parameter,

$$Q_{\alpha\alpha} = \begin{pmatrix} (\text{Re}\Psi)_x & (\text{Im}\Psi)_x & N_x \\ (\text{Re}\Psi)_y & (\text{Im}\Psi)_y & N_y \\ (\text{Re}\Psi)_z & (\text{Im}\Psi)_z & N_z \end{pmatrix}. \quad (7)$$

The columns (rows) of  $\hat{Q}$  transform as a vector under the spin (isospin)  $\text{SO}(3)$  algebra,  $[S_\alpha, Q_{\beta\gamma}] = i\epsilon^{\alpha\beta\gamma} Q_{\beta\gamma}$  ( $[I_a, Q_{\beta\gamma}] = i\epsilon^{abc} Q_{c\beta}$ ). In analogy with Eq. (5), the GL free energy near the AF-TSC phase boundary is

$$F = \frac{1}{2}(\nabla Q_{\alpha\alpha})^2 + \bar{r}Q_{\alpha\alpha}^2 + \delta r(Q_{z,\alpha}^2 - Q_{x,\alpha}^2 - Q_{y,\alpha}^2) + \tilde{u}_1 Q_{\bar{a}\alpha}^2 Q_{\bar{b}\beta}^2 + \tilde{u}_2 Q_{\alpha\alpha} Q_{\alpha\beta} Q_{\beta\alpha} Q_{\beta\beta}. \quad (8)$$

When  $\delta r = 0$  the model has full  $\text{SO}(4)$  symmetry; away from this line, it has only  $\text{SO}(3)_{\text{spin}} \times \text{SO}(2)_c$ . Derivation of the GL energy for weakly interacting Q1D electrons [21] yields Eq. (8), with  $\tilde{u}_1 = \frac{21\zeta(3)}{16\pi^2 v_f T^2}$  and  $\tilde{u}_2 = \frac{-7\zeta(3)}{8\pi^2 v_f T^2}$ .

Model (8) depends strongly on the sign of  $\tilde{u}_2$ : for  $\tilde{u}_2 < 0$ , the triplet superconductor is unitary ( $\text{Re}\Psi \propto \text{Im}\Psi$ ); for  $\tilde{u}_2 > 0$ , it is nonunitary ( $\text{Re}\Psi \times \text{Im}\Psi \neq 0$ ). We expect the unitary case to be of experimental relevance to  $(\text{TMTSF})_2\text{PF}_6$ , and we concentrate on it in the remainder of this Letter. The mean-field diagram is then composed of AF and TSC phases separated by a first order phase transition, and a disordered [normal (N)] phase separated from the other two by second order lines (Fig. 1).

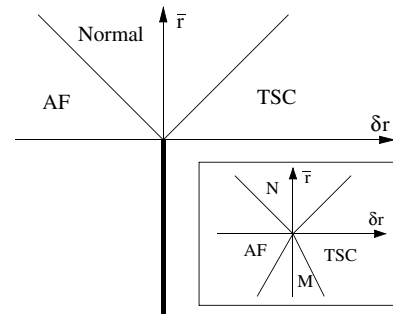


FIG. 1. Mean-field phase diagram of Eq. (8), in the unitary case  $\tilde{u}_2 < 0$ . A first order transition (thick line) divides AF and TSC phases. Inset: nonunitary case  $\tilde{u}_2 > 0$ , shown for completeness. M is a mixed (homogeneous) AF-TSC phase.

To understand the role of thermal fluctuations in model (8) and in slightly perturbed models where the quartic coefficients do not lie exactly on the SO(4) symmetric manifold, we use  $4 - \epsilon$  RG analysis. The RG equations have only two fixed points: a trivial Gaussian fixed point,  $\bar{r} = \delta r = \tilde{u}_i = 0$ , and an SO(9) Heisenberg point,  $\delta r = \tilde{u}_2 = 0$ ;  $\bar{r}, \tilde{u}_1 \neq 0$ . Figure 2 shows the RG flow in the SO(4) symmetric plane: there are runaway flows whenever  $\tilde{u}_2 \neq 0$ . The analysis can be generalized to order parameters  $\mathbf{N}$  and  $\Psi$  that are  $N$ -component vectors, in which case the  $\text{SO}(4) \approx \text{SO}(3)_{\text{spin}} \times \text{SO}(3)_{\text{iso}}$  symmetry becomes  $\text{SO}(N)_{\text{spin}} \times \text{SO}(3)_{\text{iso}}$ . We find that even in the large  $N$  limit, all flows with  $\tilde{u}_2 < 0$  are runaway flows, indicating the absence of fixed points with unitary TSC.

The absence of a fixed point in the RG flow often implies that fluctuations induce a first order phase transition, thus precluding a multicritical point in the phase diagram. In order to inspect this possibility, we study model (8) directly in 3D in the large  $N$  limit [21]. We find (inset of Fig. 3) a first order transition between AF and TSC phases along the SO(4) symmetric line  $\delta r = 0$ , in agreement with mean-field theory. A new feature of the large  $N$  limit is the first order transition between N and AF phases in the vicinity of the critical point. If we assume that the experimentally controlled pressure changes an extensive variable conjugate to  $\delta r$ , such as the volume of the system, the first order transition broadens into a coexistence region of TSC and AF. This is consistent with the experimental phase diagram of  $(\text{TMTSF})_2\text{PF}_6$  (Fig. 3). An unusual feature of the theoretical phase diagram (inset, Fig. 3) is the first order N-TSC transition. This is similar to the fluctuation-driven first order transition between normal and superfluid phases proposed for  $^3\text{He}$  by Bailin *et al.* [26]. In bulk  $^3\text{He}$ , the coherence length is very long and the transition is mean-field-like. The fluctuation region is so small that tiny discontinuities at the transition caused by fluctuations would be impossible to observe. In QID systems, the fluctuation region is expected to be large [27] and the discontinuous nature of the N-TSC transition may be experimentally accessible. This transition has been investigated through specific heat measurements in  $(\text{TMTSF})_2\text{ClO}_4$  [28]. These were interpreted as a mean-

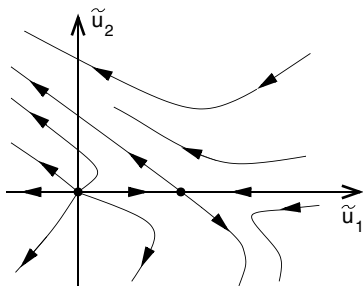


FIG. 2. The  $d = 4 - \epsilon$  RG flow of SO(4) symmetric model (8) has no stable fixed points. Instead, two types of runaway flow exist, for unitary ( $\tilde{u}_2 < 0$ ) and nonunitary ( $\tilde{u}_2 > 0$ ) TSC.

field BCS transition, although the amplitude of the specific heat jump was unusually large. Since  $T_c$  in these materials is very sensitive to impurities, the extra amplitude in the specific heat jump might be attributed to a  $\delta$ -function peak in specific heat broadened by disorder. Experimental observation of the coexistence region of N and TSC phases or of hysteresis in resistivity measurements may also be difficult: nearly equal strains in the TSC and N phases and the nearly temperature independent superconducting transition temperature can make such a coexistence region very small. Another possibility is that one loop  $4 - \epsilon$  RG calculations and the large  $N$  expansion do not capture the correct behavior of model (8) for  $\epsilon = 1$  and  $N = 3$ . De Prato *et al.* argued that a stable fixed point describing the second order N-TSC phase transition appears in a six-loop expansion [29]. We hope that future experiments will investigate the nature of the N-TSC transition in Bechgaard salts in more detail.

The most dramatic consequence of enhanced symmetry is the prediction of new low energy collective excitations. Near the AF-TSC transition, SO(4) symmetry leads to a new collective mode, corresponding to the  $\Theta$  operator that rotates AF and TSC orders into each other [21]. As pressure is tuned toward the phase transition, SO(4) becomes a better symmetry, thus decreasing the energy of the  $\Theta$  excitation. Mode softening does not occur generically at a first order phase transition and identifies the  $\Theta$  resonance as a generator of the SO(4) quantum symmetry. Weak symmetry breaking due to interchain coupling and higher order umklapp terms may lead to a small gap and to finite broadening of  $\Theta$ , even at the AF-TSC phase boundary. Deep in the normal phase,  $\Theta$  cannot be probed by conventional methods, such as electromagnetic waves or neutron scattering, as these couple only to particle-hole channels (e.g., spin or density), and  $\Theta$  is a collective mode in the particle-particle channel. The situation changes when the system becomes superconducting. Charge is not a good quantum number in the presence of a condensate of Cooper pairs, and  $p$ - $p$  and

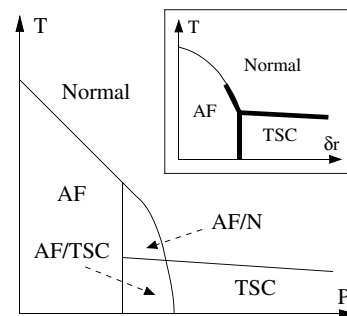


FIG. 3. Schematic temperature-pressure phase diagram of  $(\text{TMTSF})_2\text{PF}_6$  [12,13]. AF-N and AF-TSC denote coexistence regimes of the appropriate phases. Inset: phase diagram of competing AF and unitary TSC in model (8) in the large  $N$  limit. Thick lines represent first order transitions.

$p$ - $h$  channels mix.  $\Theta$  should thus appear as a resonance in inelastic neutron scattering experiments [21], with an intensity proportional to the square of the superconducting amplitude  $|\Psi|^2$ . For QID Bechgaard salts, we expect strong pairing fluctuations even above  $T_c$ . Hence, precursors of the  $\Theta$  resonance may be visible in the normal state, with a strong enhancement of the resonant scattering intensity when long range TSC order develops.

It is useful to put the SO(4) model of AF-TSC competition in Bechgaard salts in the general perspective of electron systems with competing orders. For the SO(5) theory of AF and  $d$ -wave SC in 2D systems [7,9], realistic microscopic models are difficult to construct (see, e.g., Refs. [30,31]). By contrast, SO(4) symmetry in Bechgaard salts arises naturally from a conventional Luttinger description. We also point out that the AF-TSC transition can be tuned in a single (TMTSF)<sub>2</sub>PF<sub>6</sub> sample by varying pressure, whereas tuning the AF-SC transition in the cuprates requires many different samples. Thus, we consider (TMTSF)<sub>2</sub>PF<sub>6</sub> a good candidate for experimental observation of emergence of higher symmetry in a strongly correlated electron system.

In the discussion above, we assumed Luttinger liquid behavior in individual chains to motivate the approximate SO(4) symmetry at the AF-TSC phase boundary. It has been suggested that for the superconducting phase of Bechgaard salts, interchain hopping is strong enough to turn the system into a strongly anisotropic Fermi liquid [32,33]. The decreased nesting condition in this case strongly affects antiferromagnetism. For the classical symmetry of the GL energy, this effect can be absorbed into the normalization of the field  $\mathbf{N}$ , so that the GL parameters display only a small deviation from SO(4) symmetry at the mean-field level. Thus, we do not expect a qualitative change in the phase diagram presented in Fig. 3 (see Ref. [21] for a detailed discussion). To verify the approximate quantum SO(4) symmetry for the strongly anisotropic Fermi liquid, one can study the spectrum of collective excitations using an RPA-type analysis and verify the existence of the  $\Theta$  excitation [34]. These results will be presented elsewhere.

In summary, we introduced an SO(4) framework for the competition between AF and TSC in QID electron systems. The microscopic origin of SO(4) symmetry was identified in the Luttinger liquid model. Our results have direct implications for QID organic Bechgaard salts. For example, first order transitions between AF and TSC phases, and between AF and N phases, explain the AF-TSC and the AF-N coexistence regions found in the phase diagram of (TMTSF)<sub>2</sub>PF<sub>6</sub> [12]. We also argue that the N-TSC transition in these materials could be weakly first order. We predict a sharp resonance in neutron scattering, whose characteristics identify it unambiguously as a generator of SO(4) symmetry.

We thank S. Brown, P. Chaikin, B.I. Halperin, S. Sachdev, D.-W. Wang, and S.C. Zhang for useful dis-

cussions. This work was supported by Harvard NSEC.

- 
- [1] D. Jérôme, in *Organic Conductors: Fundamentals and Applications*, edited by J. P. Farges (Marcel Dekker, New York, 1994).
  - [2] S. Lefebvre *et al.*, Phys. Rev. Lett. **85**, 5420 (2000).
  - [3] N. Mathur *et al.*, Nature (London) **394**, 39 (1998).
  - [4] Y. Kitaoka *et al.*, J. Phys. Condens. Matter **13**, L79 (2001).
  - [5] M. Maple, J. Magn. Magn. Mater. **177**, 18 (1998).
  - [6] D. J. Scalapino, Phys. Rep. **250**, 329 (1995); E. Carlson *et al.*, in *The Physics of Conventional and Unconventional Superconductors*, edited by K. H. Bennemann and J. B. Ketterson (Springer, Berlin, 2002); E. Altman and A. Auerbach, Phys. Rev. B **65**, 104508 (2002); S. Sachdev, Rev. Mod. Phys. **75**, 913 (2003).
  - [7] S. C. Zhang, Science **275**, 1089 (1997); E. Demler, W. Hanke, and S. C. Zhang, cond-mat/0405038.
  - [8] S. Murakami *et al.*, Phys. Rev. Lett. **82**, 2939 (1999).
  - [9] S. Murakami and N. Nagaosa, J. Phys. Soc. Jpn. **69**, 2395 (2000).
  - [10] D. Jérôme *et al.*, J. Phys. (Paris), Lett. **41**, 95 (1980).
  - [11] K. Andres *et al.*, Phys. Rev. Lett. **45**, 1449 (1980).
  - [12] T. Vuletic *et al.*, Eur. Phys. J. B **25**, 319 (2002).
  - [13] A. V. Kornilov *et al.*, Phys. Rev. B **69**, 224404 (2004).
  - [14] M. Choi, P. Chaikin, and R. L. Greene, Phys. Rev. B **34**, 7727 (1986); M. Choi *et al.*, *ibid.* **25**, 6208 (1982); S. Tomic *et al.*, J. Phys. (Paris), Colloq. **44**, C3-1075 (1983).
  - [15] I. J. Lee *et al.*, Phys. Rev. Lett. **78**, 3555 (1997).
  - [16] I. J. Lee *et al.*, Phys. Rev. B **68**, 092510 (2003).
  - [17] M. Takigawa *et al.*, J. Phys. Soc. Jpn. **56**, 873 (1987); H. I. Ha *et al.*, Synth. Met. **137**, 1215 (2003); N. Joo *et al.*, Eur. Phys. J. B **40**, 43 (2004); J. Oh and M. Naughton, Phys. Rev. Lett. **92**, 067001 (2004).
  - [18] R. Brusetti *et al.*, J. Phys. (Paris) **43**, 801 (1982).
  - [19] T. Giamarchi and H. J. Schulz, Phys. Rev. B **39**, 4620 (1989).
  - [20] K. B. Efetov, Sov. Phys. JETP **54**, 583 (1981); S. T. Carr and A. M. Tsvelik, Phys. Rev. B **65**, 195121 (2002); A. V. Rozhkov and A. J. Millis, *ibid.* **66**, 134509 (2002).
  - [21] D. Podolsky, E. Altman, T. Rostunov, and E. Demler, cond-mat/0409469 [Phys. Rev. B (to be published)].
  - [22] J. B. Torrance *et al.*, Phys. Rev. Lett. **49**, 881 (1982).
  - [23] C. N. Yang and S. C. Zhang, Mod. Phys. Lett. B **4**, 759 (1990).
  - [24] Y. Zhang *et al.*, Phys. Rev. B **66**, 094501 (2002).
  - [25] N. Thorup *et al.*, Acta Crystallogr. B **37**, 1236 (1981).
  - [26] D. Bailin *et al.*, J. Phys. C **10**, 1159 (1977).
  - [27] H. J. Schulz *et al.*, J. Phys. (Paris) **42**, 991 (1981).
  - [28] P. Garoche *et al.*, J. Phys. (Paris), Lett. **43**, 147 (1982).
  - [29] M. De Prato, A. Pelissetto, and E. Vicari, cond-mat/0312362 [Phys. Rev. B (to be published)].
  - [30] O. Tchernyshyov *et al.*, Phys. Rev. B **63**, 144507 (2001).
  - [31] C. L. Henley, Phys. Rev. Lett. **80**, 3590 (1998).
  - [32] V. Vescoli *et al.*, Science **281**, 1181 (1998).
  - [33] C. Bourbonnais and D. Jérôme, in *Proceedings of the International Conference of Science and Technology of Synthetic Metals (ICSM'98)* (Elsevier, New York, 1999)
  - [34] E. Demler *et al.*, Phys. Rev. B **58**, 5719 (1998).